

Metabolism of MMV669844, MMV669848 and MMV670936 in human and rat cryopreserved hepatocytes

MMV_OSDD**Report #: CDCO_MMV_OSDD_13_006****9 December, 2013****Quality Statement:**

This non-GLP study was conducted using established techniques in accordance with the relevant guidelines and standard operating procedures (SOPs) of the Centre for Drug Candidate Optimisation, Monash University. This report accurately reflects the raw data obtained during the performance of this study.

Project Leader:	Susan Charman, PhD
Project Coordinator:	Karen White, PhD
Section Leader:	Francis Chiu, PhD

Study contributors:

Analytical:	Eileen Ryan, PhD
In Vitro:	Kasiram Katneni, PhD
Study number:	MMV_OSDD_13_007

A. Study Objective

To determine the *in vitro* metabolic stability and potential metabolic products of MMV669844, MMV669848 and MMV670936 formed using human and rat cryopreserved hepatocytes.

B. Experimental Methods

Incubation Methods:

Test compounds were incubated at 37°C and 1.0 µM concentration with suspensions of human (Lot #1110211; pooled, 5 male and 5 female donors) or rat (Lot # 1110515; male Sprague Dawley, pooled, n=4 animals) cryopreserved hepatocytes (XenoTech, Lenexa, KS, USA). A relatively short incubation time of 60 minutes was used to ensure hepatocyte viability over the incubation period. The average viable cell concentration over the incubation period was determined by the Trypan Blue exclusion method in the absence of test compound and the average viable hepatocyte cell concentrations were 0.42 and 0.90 million cells per mL for human and rat, respectively.

At various time points over the 60 minute incubation, samples of hepatocyte suspension were quenched by addition of ice cold acetonitrile containing 0.15 µg/mL of diazepam as an internal standard. Concentrations of test compounds were determined by LC-MS (see below) relative to calibration standards prepared in quenched hepatocyte mixture.

To facilitate metabolite identification, additional incubations were performed at 2x the hepatocyte cell concentrations stated above and 10 µM test compound concentration, with samples being quenched at 2, 30 and 60 minutes.

Analytical Conditions:

Instrument:	Waters Micromass Xevo G2QTOF coupled to a Waters Acquity UPLC
Detection:	Positive electrospray ionisation under MS ⁺ E mode
Cone Voltage	30
Column:	Ascentis Express Amide column (50 x 2.1 mm, 2.7 µm)
LC conditions:	Gradient cycle time: 6 minutes; Injection volume: 5 µL; Flow rate: 0.4 mL/min
Mobile phase:	Acetonitrile-Water gradient with 0.05% Formic acid
Metabolite Identification	Identity of putative metabolites was confirmed by accurate mass and MS/MS fragmentation where possible
Note:	For molecular ion and retention time details for each test compound and their predicted metabolites refer to Tables 1 to 3 in Results and Discussion section

Calculations:

Test compound concentration versus time data were fitted to an exponential decay function to determine the apparent first-order rate constant for substrate depletion (k) that was then used to calculate the degradation half-life [1] and the *in vitro* intrinsic clearance, CL_{int, in vitro} [2]:

$$t_{1/2} = \frac{\ln(2)}{k} \quad [1]$$

$$CL_{\text{int, in vitro}} = \frac{k}{\text{hepatocyte cell number (10}^6 \text{ viable cells/mL)}} \quad [2]$$

Each value for $CL_{int, in vitro}$ was multiplied by a Physiologically-Based Scaling Factor (PBSF) to obtain the predicted *in vivo* hepatic intrinsic clearance, $CL_{int, in vivo}$ [3]:

$$\text{Predicted } CL_{int, in vivo} = CL_{int, in vitro} \times \text{PBSF} \quad [3]$$

PBSF values are shown in the table below and take into account the liver weight (g) per kg body weight and the hepatocellularity (10^6 cells per gram of liver) as previously described (Ring et al., 2011).

Species	PBSF ^a (10^6 cells/kg body weight)	Hepatic blood flow (Q) ^a (mL/min/kg body weight)
Human	2544.3	20.7
Rat	4684.8	67.6

^a Ring et al. (2011) *Journal of Pharmaceutical Sciences*, 100:4090-4110.

The predicted *in vivo* blood clearance (predicted CL_{blood}) was then obtained by application of the well-stirred model of hepatic elimination, without correction for binding (either *in vitro* in hepatocytes or *in vivo* in blood) [4].

$$\text{Predicted } CL_{blood} = \frac{Q \times CL_{int, in vivo}}{Q + CL_{int, in vivo}} \quad [4]$$

where Q is the nominal hepatic blood flow.

The predicted *in vivo* hepatic extraction ratio (E_H) was then calculated [5]:

$$E_H = \frac{\text{Predicted } CL_{blood}}{Q} \quad [5]$$

Hepatocyte-predicted hepatic extraction ratios (E_H) based on the relative rates of compound degradation *in vitro*, classify compounds as potentially being subject to low (< 0.3), intermediate (0.3 – 0.7), high (0.7 – 0.95) or very high (> 0.95) *in vivo* hepatic extraction.

The assumptions underlying the calculation of the *in vivo* hepatic intrinsic clearance based on the rate of degradation in hepatocytes are stated below.

NOTE:

Calculations of intrinsic clearance (CL_{int}) are based on the “*in vitro* $T_{1/2}$ method”², which assumes:

- 1) the substrate concentration employed is well below the apparent K_M for substrate turnover; and,
- 2) there is no significant product inhibition, nor is there any mechanism based inactivation of enzyme.

The use of hepatocytes in the prediction of the *in vivo* hepatic clearance and extraction ratio further assumes that hepatic metabolic clearance is the major clearance mechanism for compounds *in vivo*;

Data should be considered within these terms of reference.

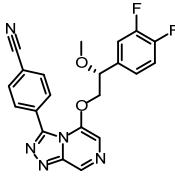
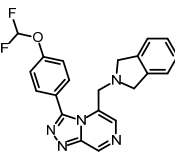
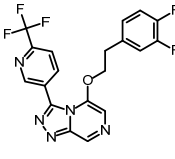
References:

- 1) Ring B.J. et al. PhRMA CPCDC Initiative on predictive models of human pharmacokinetics, part 3: Comparative assessment of prediction methods of human clearance. *J. Pharm. Sci.*, 2011, 100:4090-4110.
- 2) Obach R.S. Prediction of human clearance of twenty-nine drugs from hepatic microsomal intrinsic clearance data: An examination of *in vitro* half-life approach and nonspecific binding to microsomes, *Drug Metab. Dispos.*, 1999, 27:1350-1359.

C. Results and Discussion

Rates of degradation for MMV669844, MMV669848 and MMV670936 in human and rat cryopreserved hepatocytes correspond to moderate hepatocyte-predicted hepatic extraction ratios, and E_H values suggest that there is no significant species difference in hepatocellular metabolic stability for each compound (Table 1).

Table 1: In vitro metabolic stability parameters of three compounds based on degradation profiles in human and rat cryopreserved hepatocytes.

Compound Details (Batch #)	Species	Degradation half-life (min)	<i>In vitro</i> CL _{int} ($\mu\text{L}/\text{min}/10^6$ cells)	Hepatocyte- Predicted E_H
 MMV669844 (Free base; Batch # PCCBTAK-0190)	Human	231	7	0.47
	Rat	57	14	0.48
 MMV669848 (Free base; Batch # PCCBTAK-0194)	Human	82	20	0.71
	Rat	32	24	0.62
 MMV670936 (Free base; Batch # PCCBTAK-0272)	Human	165	10	0.55
	Rat	53	15	0.50

A metabolite search was conducted for MMV669844, MMV669848 and MMV670936 and a summary of the structure-based metabolic transformations assessed are presented in Tables 2, 3 and 4, respectively. A description of the metabolites observed is provided below and proposed structures are presented in Figures 1 to 3.

MMV669844

- A mono-oxygenated metabolite with a molecular ion 16 Daltons higher than the parent ($M+16$, $[\text{MH}^+]$ 424) was detected in both human and rat hepatocytes. MS/MS spectra indicate that the site of metabolism is most likely on the phenyl triazolopyrazine region (Figure 1) however the exact location could not be determined.
- A metabolite with an $[\text{MH}^+]$ 394 corresponding to O-demethylation (M-14) was detected in both human and rat hepatocyte incubations and its structure (Figure 1) was confirmed by accurate mass and MS/MS spectra.
- Two putative polar metabolites with an $[\text{MH}^+]$ 238 were detected in both species and whilst this mass is consistent with O-dealkylation (M-170, Figure 1), the presence of two peaks indicates that one or both of these peaks could be due to in-source fragmentation

of metabolites with a modified difluorophenyl ethyl side chain such as hydroxylation at the side chain (M-170, alternative, Figure 1). Due to weak MS signal intensity, the structure of these metabolites could not be confirmed.

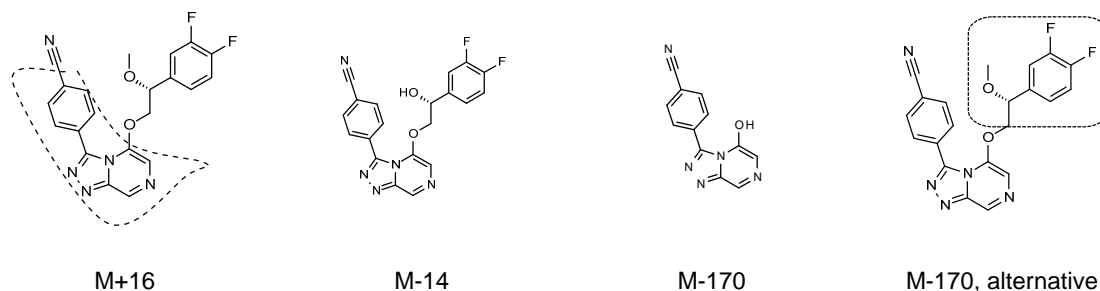


Figure 1: Proposed metabolite structures for MMV669844

MMV669848

- Two mono-oxygenated metabolites with molecular ions 16 Daltons higher than the parent (M+16 (I) & (II), [MH⁺] 410) were detected and MS/MS spectra indicate that M+16 (I), detected in both human and rat hepatocytes, is likely derived from hydroxylation at the phenyl triazolopyrazine region and M+16 (II), detected in rat hepatocytes only, at the indoline moiety (Figure 2).
- A metabolite with an [MH⁺] 390 corresponding to oxidation at the isoindoline ring (M-2) was detected in both species and its structure (Figure 2) was confirmed by accurate mass and MS/MS spectra.
- A minor metabolite with an [MH⁺] 293 corresponding to deamination cleavage of the isoindoline ring (M-101) was detected in both species and its structure (Figure 2) was confirmed by accurate mass and MS/MS spectra.
- A putative secondary metabolite with [MH⁺] 408 (M+14) was detected in both human and rat hepatocytes and is likely derived via combined mono-oxygenation and ring oxidation.
- Two putative metabolites with [MH⁺] 424 (M+30) were detected in both human and rat hepatocytes and are likely derived via a combination of the M+16 and M+14 metabolites described above.
- A putative phase II conjugate with [MH⁺] 586 (M+192) was detected in rat hepatocytes only and its accurate mass and MS/MS spectrum are consistent with glucuronidation of M+16 (II) (Figure 2).

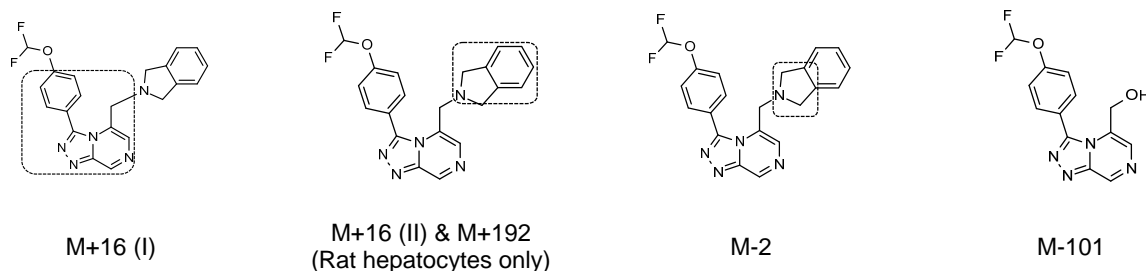


Figure 2: Proposed metabolite structures for MMV669848

MMV670936

- Three mono-oxygenated metabolites with molecular ions 16 Daltons higher than the parent (M+16 (I), (II) & (III), $[MH^+]$ 438) were detected. MS/MS spectra indicate that M+16 (I), which was detected in both species, is most likely due to hydroxylation on the difluorophenyl ethyl side chain whilst M+16 (II) and (III), which were detected in human hepatocyte incubations only, are most likely derived from oxygenation at the trifluoro triazolopyrazine region (Figure 3). In addition, it is likely that M+16 (III) is an N-oxide.
- It is possible that M+16 (II) may be due to hydroxylation of the trifluoromethylpyridine and this hydroxylation could potentially be catalysed by either aldehyde oxidase (AO) or CYP450 enzymes. However, elucidation of the exact site of hydroxylation and the enzyme system involved in its formation (i.e. AO or CYP) would require further investigation.



Figure 3: Proposed metabolite structures for MMV670936

Table 2: Potential metabolites of MMV669844 monitored in human and rat cryopreserved hepatocytes under positive ionisation mode.

Metabolite description	Δ Mass (Daltons)	MH ⁺	D/ND	t _R (min)	Metabolite Code
MMV669844	-	408	D	3.25	-
Mono-oxygenation	+16	424	D	3.00	M+16
O-demethylation	-14	394	D	2.89	M-14
O-dealkylation *	-170	238	D	M-	M-170 (I)
			D	2.20	M-170 (II)
O-dealkylation	-219	189	ND	-	-
O-dealkylation (acid)	-205	203	ND	-	-
Nitrile hydrolysis	+18	426	ND	-	-
Oxidative fluorine displacement	-2	406	ND	-	-
Bis-oxygenation	+32	440	ND	-	-
M+16 & M-14	+2	410	ND	-	-
M+16 & M-170	-154	254	ND	-	-
M+16 & Glucuronidation	+192	600	ND	-	-
M+16 & Sulphation	+96	504	ND	-	-
M-170 & Glucuronidation	+6	414	ND	-	-
M-170 & Sulphation	-90	318	ND	-	-
M-14 & Glucuronidation	+162	570	ND	-	-
M-14 & Sulphation	+66	474	ND	-	-

D = detected, ND = not detected, t_R = retention time

* whilst this mass is consistent with O-dealkylation (M-170, Figure 1), the presence of two peaks indicate that one or both of these peaks could be due to in-source fragmentation of metabolites with a modified difluorophenyl ethyl side chain such as hydroxylation at the side chain (M-170, alternative, Figure 1).

Table 3: Potential metabolites of MMV669848 monitored in human and rat cryopreserved hepatocytes under positive ionisation mode.

Metabolite description	Δ Mass (Daltons)	MH ⁺	D/ND	t _R (min)	Metabolite Code
MMV669848	-	394	D	3.16	-
Mono-oxygenation	+16	410	D	2.44	M+16 (I)
				2.56	M+16 (II) (Rat only)
O-dealkylation	-50	344	ND	-	-
N-dealkylation	-102	292	ND	-	-
Deamination	-101	293	D	2.21	M-101
Deamination (acid)	-87	307	ND	-	-
Ring dehydrogenation or Oxidative fluorine displacement	-2	392	D	3.40	M-2
Ring dehydrogenation(s) and/or Oxidative fluorine displacement(s)	-4	390	ND	-	-
Ring opening to alcohol	+18	412	ND	-	-
Bis-oxygenation or Ring opening to acid	+32	426	ND	-	-
M+16 & M-101	-85	309	ND	-	-
M+16 & M-2 or lactam formation	+14	408	D	2.82	M+14
M+16 & M+14	+30	424	D	2.53	M+30 (I)
				2.67	M+30 (II)
M+16 & Glucuronidation	+192	586	D	2.19	M+192 (Rat only)
M+16 & Sulphation	+96	490	ND	-	-
M-101 & Glucuronidation	+75	469	ND	-	-
M-101 & Sulphation	-21	373	ND	-	-
Deamination (acid) & Glucuronidation	+89	483	ND	-	-

D = detected, ND = not detected, t_R = retention time

Table 4: Potential metabolites of MMV670936 monitored in human and rat cryopreserved hepatocytes under positive ionisation mode.

Metabolite description	Δ Mass (Daltons)	MH ⁺	D/ND	t _R (min)	Metabolite Code
MMV670936	-	422	D	3.34	-
Mono-oxygenation	+16	438	D	3.05	M+16 (I)
				3.15	M+16 (II) (Human only)
				3.62	M+16 (III) (Human only)
O-dealkylation	-140	282	ND	-	-
O-dealkylation	-263	159	ND	-	-
O-dealkylation (acid)	-249	173	ND	-	-
Oxidative fluorine displacement or dehydrogenation	-2	420	ND	-	-
Bis-oxygenation	+32	454	ND	-	-
M+16 & O-dealkylation	-124	298	ND	-	-
M+16 & O-dealkylation	-247	175	ND	-	-
M+16 & O-dealkylation (acid)	-233	189	ND	-	-
Mono-oxygenation & Glucuronidation	+192	614	ND	-	-
Mono-oxygenation & Sulphation	+96	518	ND	-	-
O-dealkylation & Glucuronidation	+36	458	ND	-	-
O-dealkylation & Sulphation	-60	362	ND	-	-
O-dealkylation & Glucuronidation	-87	335	ND	-	-
O-dealkylation & Sulphation	-183	239	ND	-	-
O-dealkylation (acid) & Glucuronidation	-73	349	ND	-	-
O-dealkylation (acid) & Sulphation	-169	252	ND	-	-

D = detected, ND = not detected, t_R = retention time